DOI: 10.18721/JPM.13306
УДК 532.517

NUMERICAL MODELING OF AIR DISTRIBUTION IN A TEST ROOM WITH 2D SIDEWALL JET. II. LES-computations for the room with finite width

M.A. Zasimova[1], N.G. Ivanov[1], D. Markov[2]

[1] Peter the Great St. Petersburg Polytechnic University, St. Petersburg, Russian Federation;

[2] Technical University of Sofia, Sofia, Bulgaria

The paper presents the results of numerical modeling of turbulent airflow in a test room based on the vortex-resolving wall-modeled large eddy simulation approach. The room ventilation is provided by a plain air jet at Re = 5233. The jet is supplied from a slit placed at a side wall under the ceiling. The problem formulation reproduces the test experiment conditions (Nielsen et al., 1978, 1990) as completely as possible. Two configuration with various air supply slit width are considered. Calculations are carried out with the ANSYS Fluent software using the grid consisting of 48 million cells. The paper demonstrates that in the near-wall jet zone the computational results agree well with the experimental data, but visible disagreement is obtained in the recirculation flow region (occupied zone) with relatively low velocities.

Keywords: turbulent airflow, plain jet, large eddy simulation, ventilation

Citation: Zasimova M.A., Ivanov N.G., Markov D. Numerical modeling of air distribution in a test room with 2D sidewall jet. II. LES-computations for the room with finite width, St. Petersburg Polytechnical State University Journal. Physics and Mathematics. 13 (3) (2020) 65–79. DOI: 10.18721/JPM.13306

ЧИСЛЕННОЕ МОДЕЛИРОВАНИЕ ЦИРКУЛЯЦИИ ВОЗДУХА В ПОМЕЩЕНИИ ПРИ ПОДАЧЕ ИЗ ПЛОСКОЙ ЩЕЛИ. II. LES-расчеты для помещения конечной ширины

М.А. Засимова[1], Н.Г. Иванов[1], Д. Марков[2]

[1] Санкт-Петербургский политехнический университет Петра Великого, Санкт-Петербург, Российская Федерация;

[2] Софийский технический университет, София, Болгария

Представлены результаты численного моделирования турбулентного течения воздуха в тестовом помещении на основе вихреразрешающего подхода – метода моделирования крупных вихрей с пристенным моделированием. Вентиляция помещения осуществляется плоской воздушной струей, подаваемой из расположенного под потолком на торцевой стенке щелевого отверстия, при Re = 5233. Задача ставилась в постановке, максимально полно воспроизводящей условия тестовых экспериментов (Nielsen et al., 1978, 1990). Рассмотрены две геометрические конфигурации, отличающиеся шириной входного отверстия. Расчеты в программном пакете ANSYS Fluent выполнены с использованием сетки размерностью 48 млн. ячеек. Показано, что результаты расчетов хорошо согласуются с экспериментальными данными в пристенной струе, однако наблюдается заметное рассогласование результатов расчетов и эксперимента в зоне возвратного течения (обитаемой зоне), характеризующейся малыми скоростями.

Ключевые слова: турбулентное течение, плоская струя, метод моделирования крупных вихрей, вентиляция

Ссылка при цитировании: Засимова М.А., Иванов Н.Г., Марков Д. Численное моделирование циркуляции воздуха в помещении при подаче из плоской щели. II. LES-расчеты для помещения конечной ширины // Научно-технические ведомости СПбГПУ. Физико-математические науки. 2020. Т. 13. № 3. С. 75–92. DOI: 10.18721/JPM.13306

Introduction

A crucial factor in developing and optimizing heating, ventilation and air conditioning (HVAC) systems for residential, public and industrial buildings is organizing the air exchange ensuring comfortable microclimate for humans. The most popular methods used for simulation of air exchange are based on integral estimates and balance ratios corresponding to various conditions of supply air distribution [1]. These methods integrate empirical approaches and can be only adjusted to a specific type of flow (propagation of a free submerged jet, propagation of a near-wall jet, etc.). For this reason, balance computational methods do not always yield complete and quantitatively reliable data even for integral flow parameters in real conditions, for example, for rooms with complex geometry. Furthermore, air in applied problems is typically supplied to a room using various types of diffusers, and it is difficult to describe the characteristics of diffusers in computational methods. A complete picture of the flow, including data on the mean and local characteristics of the flow, can be gained using more accurate approaches to describing the turbulent motion of air.

Data on the spatial structure of the flow, typical for ventilation problems, which is important for substantiating design decisions, can be obtained by numerical modeling of multidimensional fluid dynamics problems. One of the most common approaches to numerical modeling of turbulent flows is solving steady/unsteady Reynolds-averaged Navier–Stokes equations (often referred to as RANS/URANS in literature) [2], closed by a semi-empirical turbulence model. Notably, the available studies on free jet flows suggest that two-parameter k-ε turbulence models [3], as well as Sekundov's model [4] with one differential equation return satisfactory results; however, validation of RANS data for simulation of complex jet flows remains a pivotal challenge.

Eddy-resolving approaches are methods for predicting the parameters of turbulent flows, have high accuracy, making it possible to obtain not only averaged but also instantaneous fields of physical quantities. The classical eddy-resolving approaches include, first of all, the direct numerical simulation method (DNS) based on directly solving the full Navier–Stokes equations. Another eddy-resolving approach is Large Eddy Simulation (LES), solving the filtered Navier–Stokes equations, which allows to resolve large eddies but requires semi-empirical modeling of small-scale eddies.

Eddy-resolving approaches have extremely high computational costs; however, the LES approach takes less computational resources compared to DNS, especially if there is no goal to resolve the near-wall regions and the simulation is limited to applying techniques based on the RANS approach. Hybrid RANS-LES approaches, including Wall Modeled LES (WMLES) have seen rapid advances over the past two decades. For example, eddy-resolving approaches are described in [5, 6].

The degree of uncertainty for the eddy-resolving LES and RANS-LES models, as well as for other approaches to modeling turbulence including some empiricism can be estimated by solving test problems for which reliable and well-described experimental data are available.

This study presents the results of validation computations for the well-known test problem of ventilation flow in a room where an air jet is supplied from a slit located under the ceiling [7, 8]. A series of laboratory experiments described in [7, 8] was aimed at studying turbulent air flow in the model of a ventilated room. Laser Doppler anemometry (LDA) was used for measuring the velocity fields and fluctuation characteristics with controlled accuracy. The measurement data are well documented: they are represented graphically in [7, 8] and available as a database at http://www.cfd-benchmarks.com/.

This paper continues the investigation in [9], where technique involving the WMLES approach was tested for computations in a simplified periodic statement. In contrast to [9], we consider the full statement of the problem, including the side walls and most accurately reproducing the experimental conditions.

Table

Studies with numerical simulation of experiment in [7]

No.	Authors	Year	Country	Method	Code	Computational Grid
2D problem statement						
[10]	Heikkinen, Piira	1991	Finland	RANS (*k*-ε)	WISH	28 × 17, 45 × 26
[11]	Vogl, Renz	1991	Germany	RANS (*k*-ε)	Fluent	56 × 62
[12]	Skalicky, Morgenstern, Auge, Hanel, Rosler	1992	Germany	RANS (*k*-ε)	Psiom2D ResCUE	64 × 32, 128 × 64
[14]	Chen	1995	USA	RANS (*k*-ε) *k*-ε RNG)	PHOENICS	50 × 45, 100 × 70
[15]	Chen	1996	USA	RANS (*k*-ε; RSTM –IP, –GY, –QI)	PHOENICS	50 × 45
[16]	Peng, Davidson, Holmberg	1996	Sweden	RANS (LRN *k*-ε)	CALC-BFC	50 × 47, 102 × 132
[19]	Bennetsen	1999	Denmark	RANS (*k*-ε, *k*-ω, ASM, DSM)	CFX 4.2	72 × 48, 144 × 96
[20]	Voight	2001	Denmark	RANS (*k*-ε, RNG, LS; *k*-ω, SST)	EllipSys	192 × 128, 288 × 192
[23]	Mora, Gadgil, Wurtz	2003	USA, France	RANS (*k*-ε) Zonal models: PL, PL-SDF, SD-SDF	SPARK Star CD	10 × 10, 40 × 40
[25]	Rong, Nielsen	2008	Denmark	RANS (*k*-ε; *k*-ω, BSL, SST)	CFX 11.0	4,736, 18,944, 28,800 cells
[26]	Dreau, Heiselberg, Nielsen	2013	Denmark	RANS (*k*-ε) low-Re, realizable; *k*-ω, SST)	CFX 11.0 Star-CCM+	4,068, 4,793, 16,658 cells
[29]	Yuce, Pulat	2018	Turkey	RANS (*k*-ε; *k*-ω)	Fluent 16.2	4,000–43,100 cells
3D problem with periodic condition						
[13]	Rosler, Hanel	1993	Germany	RANS (*k*-ε)	ResCUE	64 × 28 × 4, 128 × 48 × 4
[20]	Voight	2001	Denmark	RANS (*k*-ε LS, *k*-ω, *k*-ω BSLREV)	EllipSys	96 × 64 × 16
[27]	Ivanov, Zasimova	2018	Russia	WMLES S-Omega	Fluent 16.2	751×252×250
3D problem statement						
[17]	Davidson, Nielsen	1996	Sweden Denmark	LES (Smagorinsky, dynamic Germano)	SLAP	72 × 42 × 52, 102 × 52 × 52
[18]	Davidson	1996	Sweden	RANS (*k*-ε), LES (Smagorinsky, dynamic Germano)	CALC-BFC	72 × 42 × 52, 102 × 52 × 52
[19]	Bennetsen	1999	Denmark	RANS (*k*-ε, RNG; *k*-ω, ASM, DSM), LES (MS, Smagorinsky, dynamic Germano	CFX 4.2 LESROOM	96 × 64 × 32, 84 × 72 × 72 (RANS) 64 × 64 × 32, 96 × 64 × 64 (LES)

Continued

No.	Authors	Year	Country	Method	Code	Computational Grid
[20]	Voight	2001	Denmark	RANS (k-ε LS, k-ω BSLREV), LES (Mixed Scale, Smagorinsky,	EllipSys	96 × 64 × 16 (RANS) 72 × 48 × 36, 96 × 64 × 48 (LES)
[21]	Jiang, Chen	2001	USA	LES (Smagorinsky, Filtered Dynamic, Small-Scale model)	PHOENICS	66 × 18 × 34, 66 × 34 × 34
[22]	Jiang, Mingde, Chen	2003				
[24]	Ivanov	2005	Belgium Russia	RANS (k-ε) LS; SA)	SINF, FINE	37 × 41 × 29, 73 × 81 × 57
[27] [28]	Ivanov, Zasimova	2018	Russia	WMLES S-Omega	Fluent 16.2	751×252×250
[30]	Van Hoof, Blocken	2019	Belgium	RANS	Fluent 15.0	212,160–1,697,280 cells

Notations: RSTM is the Reynolds Stress Models [6], LRN is the Low Reynolds Number correction, BSL is Baseline revised, LS is the Launder Sharma k-ε model, ASM is the Algebraic Stress Model, DSM is the Differential Reynolds Stress Model.

Since experimental data in [7] were first published, multiple attempts have been made to reproduce the qualitative picture of the flow and quantitative data on the velocity profiles using the methods of computational fluid dynamics. Aside from the actual experimental data, the CFD Benchmarks website contains the best known computational data obtained by various scientific groups from 1991 to 2013 for the conditions corresponding to the test [7]. Notably, no results of numerical simulation are available in literature for the conditions of the experiment described in [8] with a smaller width of the inlet slit.

The table contains brief information about the studies [10—30] giving the results of numerical modeling of air exchange in a room model close to the data in [7]. The calculations were carried out in two-dimensional, quasi-two-dimensional (imposing periodic conditions in the transverse direction) and three-dimensional statements. These studies describe in detail the computational results, establishing the influence of turbulence models and various numerical parameters on the obtained solution.

The table provides data on the general dimensions of the computational grids used in numerical computations described in [10—30]. Naturally, the dimensions of the grids gradually increase over time: for example, the coarse computational grid used in computations in 1991 consisted of 100 control volumes, while the finest grid consists of approximately $4.8 \cdot 10^7$ cells (2018).

It is evident from the data in the table that the model problem was numerically solved both using the RANS approach, closed by semi-empirical turbulence models (such as k-ε, k-ω, k-ω SST, etc.), and using the eddy-resolving LES approach in combination with different subgrid-scale models. Until recently, only three research groups (Davidson et al. [17, 18], Bennetsen [19], Voight [20]) performed computations for the model problem [7] using the LES approach; however, the computational grids were very rough by modern standards (with dimensions of less than half a million cells). Importantly, it is now clear [9] that such grids do not allow to describe the behavior of three-dimensional turbulent structures with a sufficient degree of accuracy for the given problem.

Generalizing the results of numerical simulation available in literature for the experimental conditions in [7], we can conclude that the general picture obtained for the averaged flow agrees with the experiment but the local characteristics turn out to be inaccurate. It is now possible to run accurate numerical simulations of turbulent flows on fairly refined grids (with dimensions up to 10^7—10^8 cells) based on different eddy-resolving approaches, including WMLES.

This study presents the results of numerical simulation of turbulent airflow in a closed room using the eddy-resolving WMLES approach for the conditions approximating the experiments in [7, 8].

Problem statement

Room geometry. We considered airflow in a room shaped as a rectangular parallelepiped with the dimensions $3H \times H \times H$. The room is shown schematically in Fig.1, *a,* the origin of the coordinate system is located in the bottom corner of the room. The height of the room $H = 3$ m was taken as the length scale.

The inlet to the computational domain was located on the side wall of the room, under the ceiling; this inlet was an air slit with the width w_{in} and the height $h_{in} = 0.056H = 0.168$ m. In accordance with different experimental conditions in [7, 8], two geometric configurations with different inlet widths were considered.

In the first scenario, the slit width coincided with the room width, $w_{in} = H$; this statement of the problem corresponds to the experimental conditions in [7].

In the second scenario, the width of the slit was halved and was equal to $w_{in} = 0.5H$, the slit was located in the center relative to the side walls of the room (see Fig. 1,*a*); this statement corresponds to the experimental conditions in [8].

A rectangular exhaust slit with the width H and the height $h_{out} = 0.16H = 0.48$ m was located on the opposite side wall, near the floor, discharging air from the room. An outlet ventilation duct shaped as a rectangular parallelepiped with the dimensions $0.50H \times 0.16H \times 1.0H$ was installed adjacent to the slit in order to prevent backflow generated on the surface of the exhaust slit.

The experimental data from [7, 8] are available along the lines marked with dashes in Fig. 1,*a*. Vertical lines *A-A* are located at $x = 1.0H$, and *BB* at $x = 2.0H$; horizontal lines *C-C* are located at $y = 0.972H$ (at a distance $h_{in}/2$ from the ceiling, which corresponds to the midsection of the inlet slit), and *D-D* at $y = 0.028H$ (at a distance $h_{in}/2$ from the floor). The subscripts '1' correspond to the central section of the room ($z = 0.5H$), and '2' to the lateral section ($z = 0.1H$).

Notably, the laboratory experiments in [7, 8] were carried out in a scaled-down model of the room to reduce the errors in measuring the velocity: the width and height of the model were the same and were $H = 0.0893$ m, and the length was 0.268 m. However, the descriptions in [7, 8] and in subsequent numerical studies were given for the data scaled to full-size conditions.

Boundary conditions. The problem is considered in the isothermal approximation, which corresponds to the experimental conditions, where a uniform temperature field was maintained in the room. A model of incompressible fluid with constant physical properties was used to describe isothermal motion of air: density $\rho = 1.23$ kg/m^3, dynamic viscosity $\mu = 1.79 \cdot 10^5$ Pa·s.

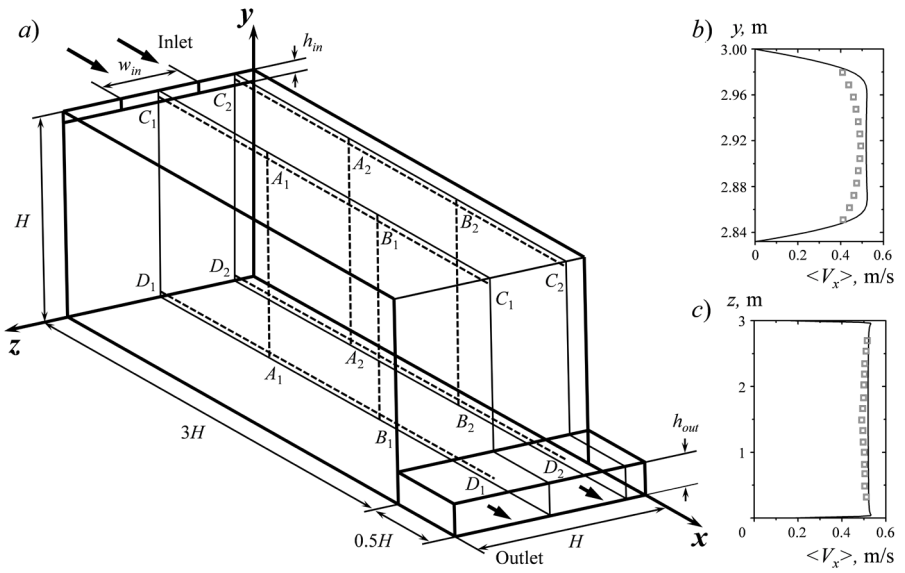

Fig. 1. Geometric model of the room (*a*). Experimental data are available along the additional lines shown; the lines and the symbols correspond, respectively to computed and experimental distributions of longitudinal velocity at the entrance to the room along two axes (*b*, *c*) for the scenario with $w_{in} = 3$ m; sections at $z = 3.000$ m (*b*) and $y = 2.916$ m (*c*) are shown

Air is supplied to the entrance to the room at an average velocity equal to $V_{in} = 0.455$ m/s (this value corresponds to a volumetric flow rate of 825 m^3/h for the first scenario with a wide inlet slit). The Reynolds number computed from the height of the inlet slit is $\mathrm{Re} = \rho h_{in} V_{in}/\mu = 5.23 \cdot 10^3$.

The experimental velocity distributions in the inlet section along the central longitudinal and transverse lines are shown by symbols in Figs. 1, *b*, *c*. We should note that the inlet ventilation duct is not described in [7, 8], which is to say that no data was provided for how the inlet velocity field was generated.

The inlet velocity profiles were extracted from an additional WMLES solution to the corresponding problem of airflow in a straight ventilation duct with the dimensions $L_{duct} \times h_{in} \times w_{in}$. The duct length was taken equal to $L_{duct} = 2.0H = 6$ m, and its cross section corresponded to the inlet slit with the dimensions $h_{in} \times w_{in}$.

Soft boundary conditions were imposed at the exit boundary of the computational domain. The remaining boundaries of the computational domain were solid walls where no-slip conditions were imposed.

Mathematical model. Turbulent air flow was simulated using the eddy-resolving WMLES approach, which is based on solving the filtered Navier–Stokes equations (see, for example, [31]). By applying the filtering procedure, the instantaneous variables f in the Navier–Stokes equations are replaced by the sum of filtered and subgrid-scale variables $f = \tilde{f} + f'$. The quantity $\tilde{f}$ is determined by the expression

$$\tilde{f}(x,t) = \int_{Vol} G(x - x', \Delta) f(x', t) dx'^3, \qquad (1)$$

where $G(x - x', \Delta)$ is the filtering function determining the size and structure of small-scale turbulence (for example, a box filter); x, m, is the coordinate of the given point, Δ, m, is the characteristic size of the filter (filter width).

Eddies whose size is smaller than the filter width are not resolved.

The filtered equations for incompressible fluid with constant physical properties can be written in the following form:

$$\begin{cases} \nabla \cdot \mathbf{V} = 0; \\ \dfrac{\partial \mathbf{V}}{\partial t} + \nabla \cdot (\mathbf{V}\mathbf{V}) = \\ = -\dfrac{1}{\rho} \nabla \cdot p + 2\nu (\nabla \cdot \underline{S}) - \nabla \cdot \underline{\tau}^{\mathrm{SGS}}, \end{cases} \qquad (2)$$

where $\mathbf{V}$ is the velocity vector with the components (V_x, V_y, V_z); $\underline{S}$ is the strain rate tensor; $\underline{\tau}_{\mathrm{SGS}}$ is the term resulting from spatial filtering of the equations.

The generalized Boussinesq hypothesis is used to determine the subgrid-scale stresses:

$$\tau_{ij}^{SGS} - \frac{1}{3} \tau_{kk} \delta_{ij} = -2\nu_{SGS} S_{ij}, \qquad (3)$$

where ν_{SGS} is the subgrid-scale turbulent viscosity to be determined using some semi-empirical subgrid model.

The WMLES S-Omega approach implemented based on the data in [32] was used in the computations. Compared with the standard Smagorinsky model, the subgrid-scale viscosity is determined using a modified linear subgrid scale, a damping factor (similar to the Van Driest factor in the Prandtl model for the RANS approach), and the difference $|S - \Omega|$ instead of the magnitude of the strain-rate tensor S:

$$\nu_{SGS} = \min \left\{ (\hat{e} d_w)^2, (C_S \Delta)^2 \right\} \times |S - \Omega| \times \\ \times \left(1 - \exp \left\{ \left(-y^+ / 25 \right)^3 \right\} \right), \qquad (4)$$

where $C_S = 0.2$ is the empirical Smagorinsky constant; S, s^{-1}, Ω, s^{-1}, are the magnitudes of strain rate and vorticity tensors

$$(S = (2S_{ij}S_{ij})^{0.5}, \Omega = (2\Omega_{ij}\Omega_{ij})^{0.5});$$

$\kappa = 0.41$ is the Kármán constant; d_w, m, is the distance to the nearest wall, y^+ is the normalized distance from the center of the first wall cell to the wall.

The quantity Δ is determined by the formula

$$\Delta = \min \{ \max(C_w d_w, \\ C_w \Delta_{\max}, \Delta_{wn}), \Delta_{\max} \}, \qquad (5)$$

where $\Delta_{\max}$, m, is the maximum grid cell size (found as the maximum edge length for an orthogonal hexagon); Δ_{wn}, m, is the grid step along the normal to the wall; $C_w = 0.15$ is an empirical constant.

Since only averaged values were extracted from the solution of the auxiliary problem on air flow in a flat channel to impose the inlet boundary conditions, one of the available synthetic turbulence generators, the Vortex Method [33], was used to determine the instantaneous fluctuation characteristics (turbulent content) in the inlet section. With the synthetic turbulence generator engaged, it is required to determine

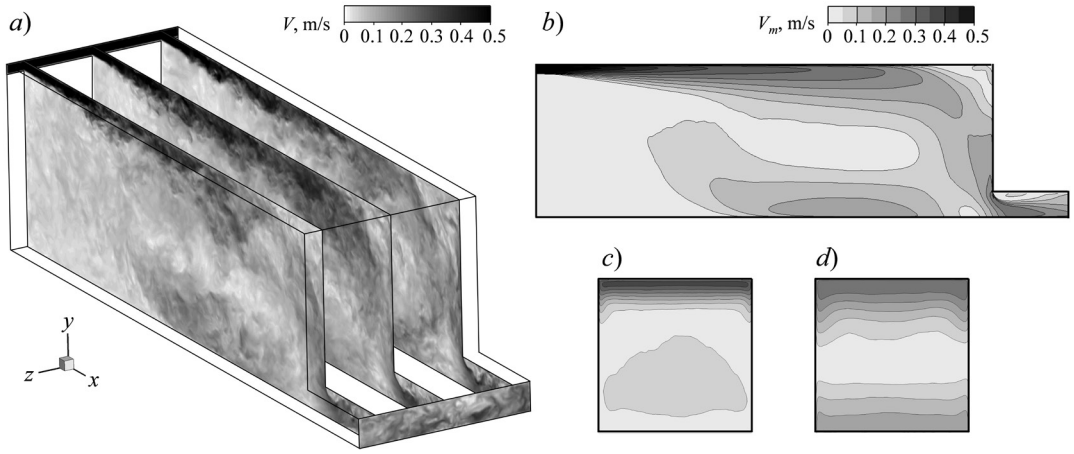

Fig. 2. Instantaneous velocity fields in vertical sections z = 0.3 m, 1.5 m and 2.7 m of the room model (*a*); fields of mean velocity magnitude in sections z = 1.5 m (*b*), x = 3.0 m (*c*) and x = 6.0 m (*d*)

the turbulence intensity at the inlet boundary; the value I = 4% was given.

Computational aspects of the problem. Numerical modeling was carried out in the ANSYS Fluent 16.2* general-purpose hydrodynamic code, with discretization of the governing equations by the finite volume method. A uniform grid consisting of cubic elements and built in the ICEM CFD generator was used. The grid dimension was approximately 48 million cells (751 × 252 × 250), while the linear size of the cell was Δ = 12 mm.

The parameters selected for the computational algorithm provided spatial and temporal discretization with second-order accuracy. The central differencing scheme was used for approximating the convective terms in the equation of motion. The non-iterative algorithm corresponding to time advancement by the method of fractional steps (NITA) was used. The time step Δt, equal to 0.01 s, was chosen so that the maximum value of the Courant number in the computational domain was less than unity. Additional computations confirmed that a decrease in the time step to 0.006 s does not affect the averaged flow characteristics. The rationale for the choice of the grid and other aspects related to applying the LES method are considered in the first part of this study [9], considering a periodic problem with no influence from the side walls.

The development of unsteady flow was controlled by placing monitoring points in different positions in the room, allowing to detect the transition to a statistically steady flow regime. Notably, the fluctuation characteristics of the flow are highly sensitive to the length of the averaging interval. Samples from 1500 s (150,000 time steps) to 3,000 s were computed to accumulate representative statistics. The averaged characteristics computed over shorter averaging periods turned out to be significantly dependent on the sample.

The computations were carried out using the resources of the Polytechnic Supercomputer Center (http://www.scc.spbstu.ru). The problems were run on the Polytechnic RSC Tornado cluster with a peak performance of 943 teraflops. The cluster contains 668 dual-processor nodes (Intel (R) Xeon (R) E5 2697v3), each node containing 14 cores. A problem was run on a maximum of 512 parallel cores, while it took at least three weeks of real time (258,000 core hours) to accumulate unsteady statistics.

Computational results and discussion

Description of the flow structure (scenario 1, $w_{in} = H$). The structure of the flow in the room is illustrated in Fig. 2, showing the instantaneous, i.e.,

$$V = (V_x^2 + V_y^2 + V_z^2)^{0.5},$$

and averaged, i.e.,

$$V_m = (\langle V_x \rangle^2 + \langle V_y \rangle^2 + \langle V_z \rangle^2)^{0.5},$$

fields of the velocity magnitude for the first computational scenario, with the width of the inlet slit coinciding with the width of the room ($w_{in} = H$), in several sections of the room. The symbols ‹...› here and below refer to time averaging.

A near-wall turbulent jet of air develops near the ceiling (the upper regions of the fields in Fig. 2), which is practically symmetric

* ANSYS Inc. ANSYS Fluent 16.2 User's Guide, 2015.

relative to the midsection of the room. As the jet propagates from the inlet slit to the opposite side wall, the velocities approximately halve (from V_{in} = 0.455 to 0.200 m/s). Colliding with the wall opposite to the entrance, the jet turns around, and a secondary low-velocity flow is generated in the bottom of the room, characterized by velocities less than 0.1 m/s.

As follows from the flow patterns in the cross sections (see Fig. 2, *c*, *d*), the flow in most of the room is uniform along the transverse *z*-direction, even though the cross section of the room is a square (W/H = 1). Pronounced deviations from the two-dimensional (planar) structure of the flow are observed near the side walls of the room, as well as in the region of lower velocities of recirculation flow. Thus, a simplified statement of the problem with the periodic condition imposed makes it possible to predict the structure of the flow; however, as established in [9], the periodic computational domain has to sufficiently extended in the transverse direction for this purpose, i.e., $W/H \geq 1$.

The pattern of the flow in the midsection (see Fig. 2, *b*) indicates that two regions with substantially different scales are observed in the room: the jet flow zone, i.e., the region where an intense near-ceiling jet develops, with characteristically high air velocities, and the occupied zone with low-velocity circulation flow, which is where fresh air is supplied to people in the room in real-world conditions. It is rather difficult to describe such a flow by numerical modeling because the flows evolving in different areas of the room have different scales.

The data obtained at the monitoring points located in the jet flow zone also point to multiscale flow (point *A* with coordinates 3.0, 2.8 and 1.5 m) and recirculation flow (point *B* with coordinates 3.0, 0.4 and 1.5 m); Fig. 3,*a* shows the evolution of the longitudinal velocity component at these points.

High-frequency fluctuations are observed in the jet flow zone, with their amplitude comparable to the mean velocity ($\langle V_x \rangle$ = 0.29 m/s for the point *A*, and the value of the maximum deviation from this average equals 0.27 m/s). The characteristic time scale of the fluctuations at the point *A* is less than 5 s. The relative amplitude of the fluctuations is much higher in the region of lower velocities; the characteristic time scale of low-frequency oscillations also turns out to be an order of magnitude higher than in the jet flow zone, for example, it is about 150 s at the point *B*.

Fig. 3,*b* shows the frequency dependence of the power spectral density (PSD), calculated from the *x*-velocity component (see Fig. 3,*a*), which was obtained using the formula

$$\mathrm{PSD} = 2A_{Ux}{}^2\Delta t,$$

where A_{Ux} is the amplitude of harmonic components in the Fourier transform.

A straight line added to the graph reflects the decrease in the spectrum by the Kolmogorov law (denoted as the "−5/3 law"). This law states that the frequency power spectrum exhibits universal behavior in the inertial range $E \sim k^{-5/3}$, where E is the spectral power density of kinetic energy, k is the wavenumber. A region where the Kolmogorov law is satisfied can be observed on the spectral curves plotted from the data at the points *A* and *B*. The graphs also show that the energy spectra of fluctuations are filled for more than two decades, which indicates that the given flow is described by a regime with developed turbulence.

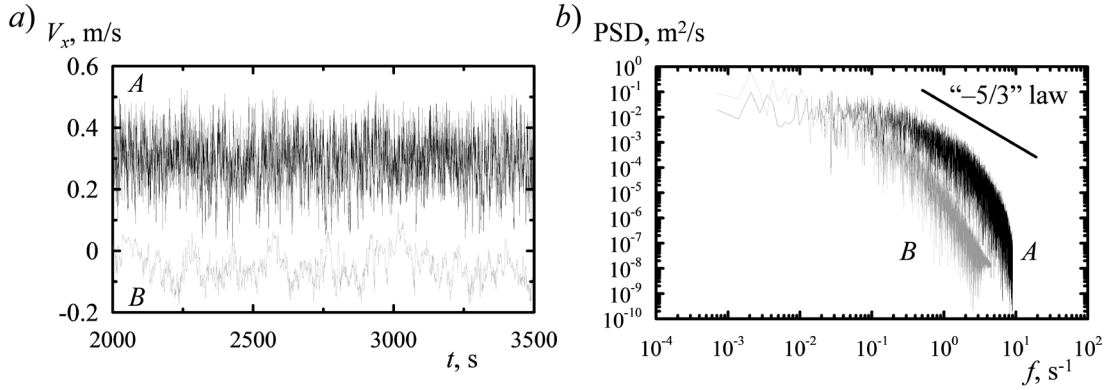

Fig. 3. Time history of *x*-velocity components at two monitoring points: point *A* with coordinates (3.0, 2.8 and 1.5 m) and point *B* (3.0, 0.4 and 1.5 m) (*a*); energy spectra of velocity fluctuations at these points

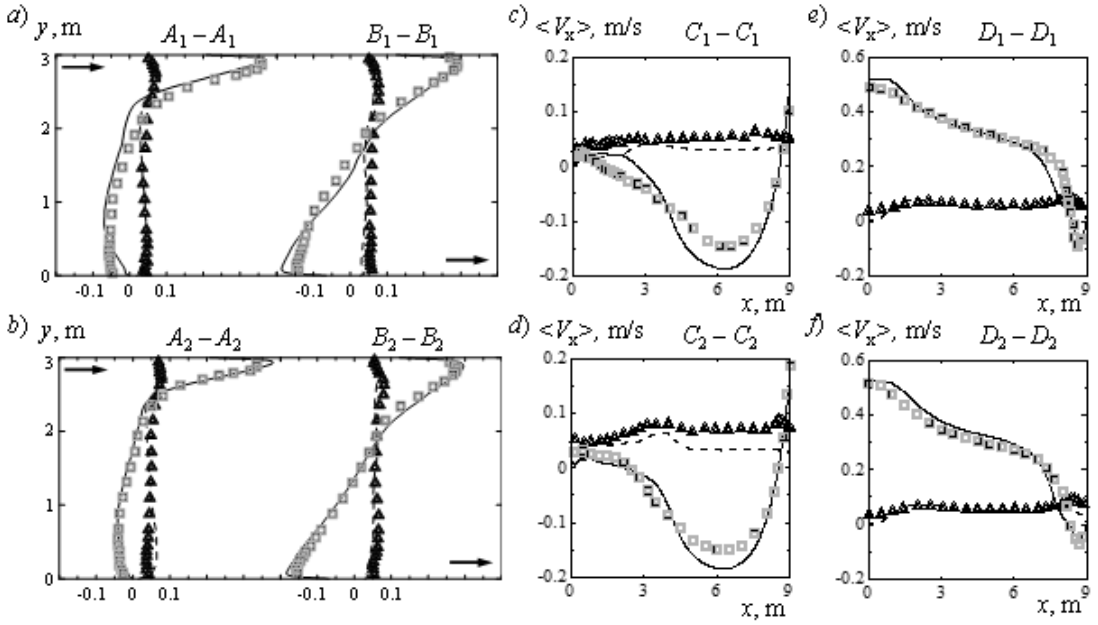

Fig. 4. Computed (solid lines) and experimental (squares) velocity profiles; profiles of velocity fluctuations (dashed lines and triangles, respectively) in several sections of the geometric model of the room (see Fig. 1,*a*)

Comparison with experimental data (scenario 1, $w_{in} = H$). Fig. 4 shows the profiles of the time-averaged x-velocity component $\langle V_x \rangle$, and its root-mean-square deviations from the mean value $(\langle V_x'^2 \rangle)^{0.5}$ in eight sections (lines) of the room (see Fig. 1,*a* for the locations of sections). The graphs summarize the data obtained in the course of this numerical simulation and experimental data given in [7]. The top of Fig. 4 shows graphs along the lines drawn in the central section of the room, the bottom shows lines in the lateral section. It is evident from the graphs that the flow in the room is quasi-two-dimensional in a wide range of transverse coordinates (as noted above); the profiles of velocity and its fluctuations in the central and lateral sections are identical both qualitatively and quantitatively.

The results of numerical computations are in good agreement with the experimental data in the region of the near-ceiling jet. At the same time, there is a disagreement between the computational and experimental results in the backflow zone. The computed profiles of velocity and its fluctuations in vertical sections (lines *A-A* and *B-B*) adequately reproduce the experimental data; there is some discrepancy in the results in the vicinity of the room's floor at $y < 1$ (see Fig. 4,*a*,*b*). A certain disagreement between the computed and experimental results can also be observed from the data for velocity and its fluctuations in the horizontal sections of the room located in the backflow zone (lines *C-C* in Fig. 4, *c*, *d*), where local maxima of the velocity appear. Conversely, the computations are in good agreement with the experiment along the horizontal lines *D-D* (see Fig. 4, *e*, *f*).

Comparing the results with the data obtained earlier by other authors, numerically simulating the experimental conditions in [7] (see Table 1), we can conclude that the results of these studies are in better agreement with the experimental data [7] both in terms of velocity profiles and fluctuation characteristics. This is particularly pronounced in the jet flow zone (sections *D-D* in Fig. 4, *e*, *f*), for which quantitative agreement of the computational and experimental data was obtained in this study, and the position of the point where the jet separates from the top wall was predicted accurately. Our computations predict more intense flow than was observed in the experiment for the region of secondary flow (sections *C-C* in Fig. 4, *c*, *d*): the values of velocity and its fluctuations prove to be overestimated by the computational data. All studies published previously by other authors pointed to a significant disagreement between the computations and the experiment in the backflow zone with relatively low velocities.

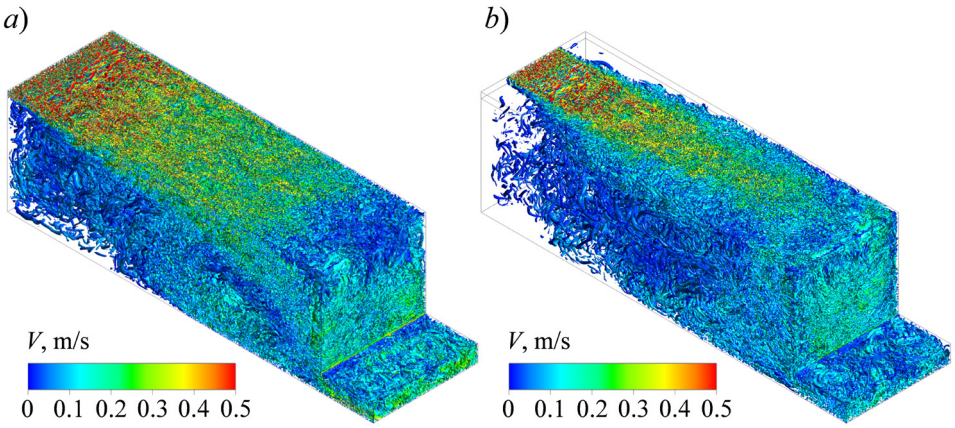

Fig. 5. Instant isosurfaces of Q criterion, colored by velocity magnitude; constructed for two computational scenarios: $w_{in} = H$ (*a*) and $0.5H$ (*b*)

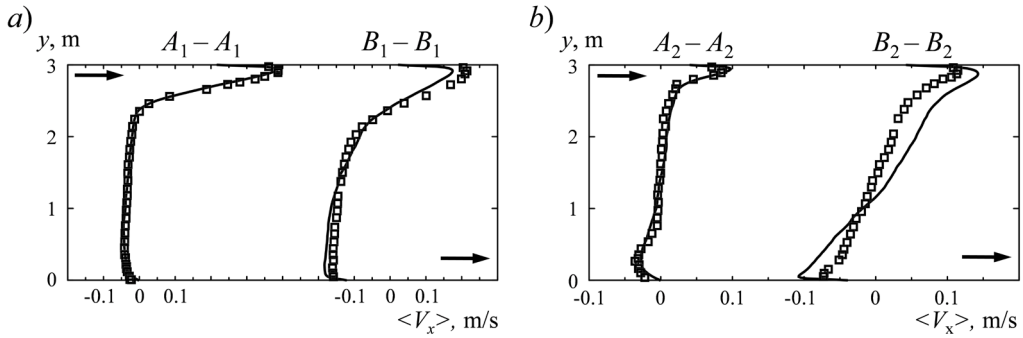

Fig. 6. Computed (solid lines) and experimental [8] (symbols) profiles of longitudinal velocity component in sections *A-A* and *B-B* for scenario 2, $w_{in} = 0.5H$

Characteristics of the flow with decreasing width of the inlet slit (scenario 2, $w_{in} = 0.5H$). Fig. 5 shows the characteristics of the flow for scenario 2, where the width of the inlet slit is half the width of the computational domain; the flow structures in both scenarios are compared. The figure shows three-dimensional isosurfaces of the Q criterion taking the form $Q = 0.5(\Omega^2 - S^2)$, where Q has a value equal to 0.1 s^{-2}; the colors of the isosurfaces correspond to the values of the velocity magnitude. As the width of the inlet slit is halved, additional mixing layers evolve in the transverse (z) direction; their development is noticeable in the near-ceiling zone in the corners of the room: the averaged flow exhibits a fundamentally three-dimensional nature here. The differences in the patterns of jet propagation are smoothed out away from the entrance; the numerical solutions demonstrate practically the same distributions of the Q criterion in the region where the jet ineracts with the opposite side wall.

On the whole, it can be concluded that the global structure of the flow is identical for the two scenarios differing by the width of the inlet slit, except for the region in the vicinity of the entrance.

Fig. 6 compares the time-averaged profiles of the x velocity components obtained in the computations with the experimental data from [8] along the vertical lines *AA* and *B-B* (note that only a very limited set of experimental data is available for the problem with the smaller widths of the inlet slit). Fig. 6,*a* shows the distributions along the lines in the central section, with $z = 1.5$ m; Fig. 6,*b* shows the distributions along the lines in the lateral section, with $z = 0.3$ m (this value of the transverse coordinate is already outside the inlet slit). The graphs confirm that the computational results are in complete agreement with the experimental data in the near wake (lines *A-A*). Differences between the computed and experimental velocity

profiles in the area of the room located closer to the exit (lines *B*-*B*), especially in the lateral section. The reasons for disagreement may stem both from the drawbacks of the numerical simulation technique and from the uncertainty of the experimental data given in [8]. We should note that the computations revealed a strong sensitivity of the averaged flow characteristics to the duration of the sample used for averaging: independence from the averaging interval was achieved in the computations (for the samples exceeding 1500 s).

The computations indicate that using a sufficiently long sample for averaging is of fundamental importance for an averaged flow with a substantially three-dimensional pattern, characteristic for scenario 2. There is no information about the averaging technique (including the duration of the samples) used in the experiments in [7, 8]. It is also known that the errors in velocity measurements can sharply increase in the region of low-velocity flow: specifically, a greater disagreement between the computational and experimental data is observed in this region.

Conclusion

The eddy-resolving WMLES approach was used in this study for numerical simulation of turbulent air flow in a room with a square cross-section ventilated by a plain air jet supplied from a slit located under the ceiling; the Reynolds number $Re = 10 \cdot 5^3$. The problem was formulated in a statement that most fully reproduced the conditions of the test experiment. Two geometric configurations were considered, differing by the width of the inlet slit. The computations were carried out in the ANSYS Fluent general-purpose CFD code, providing second-order spatial and temporal discretization.

Despite the geometric simplicity, the flow evolving in the room combines many factors that complicate the simulations:

a plain near-wall jet develops under the ceiling of the room;

after turning around, the descending jet flows onto the lower wall;

the side walls play a certain role, forming the three-dimensional structure of the averaged flow.

We have established that the computational results are in good agreement with the experimental data in the near-wall jet, however, there is a noticeable discrepancy between the computational results and the experiment in the backflow zone (occupied zone), which is characterized by relatively low velocities.

Acknowledgment

We would like to express our gratitude to the Andrey Garbaruk (associate professor of Peter the Great St. Petersburg Polytechnic University) and Vladimir Ris (director of Scientific and Educational Center for Computer Technologies in Aerodynamics and Thermal Engineering of Peter the Great St. Petersburg Polytechnic University) for valuable advice and comments.

This study was supported by the Academic Excellence Project 5-100 proposed by Peter the Great St. Petersburg Polytechnic University.

REFERENCES

1. **Grimitlin M.I.,** Raspredelenie vozdukha v pomeshcheniyakh [Air distribution in the rooms], 3rd Ed., AVOK Severo-Zapad, St. Petersburg, 2004 (in Russian).

2. **Reynolds O.,** IV. On the dynamical theory of incompressible viscous fluids and the determination of the criterion, Phil. Trans. Roy. Soc. Mathematical, Physical and Engineering Sciences. 186 (December) (1895) 123–164.

3. **Launder B.E., Spalding D.B.,** Lectures in mathematical models of turbulence, Academic Press, London, New-York, 1972.

4. **Guliaev A.N., Kozlov V.E., Sekundov A.N.,** A universal one-equation model for turbulent viscosity, Fluid Dynamics. 28 (4) (1993) 485–494.

5. **Sagaut P.,** Large Eddy Simulation for incompressible flows: An introduction, 3rd Ed., Springer, Heidelberg, 2006.

6. **Garbaruk A.V., Strelets M.Kh., Travin A.K., Shur M.L,** Sovremennyye podkhody k modelirovaniyu turbulentnosty [Modern approaches to turbulence modelling], St. Petersburg Polytechnic University Publishing, St. Petersburg, 2016 (in Russian).

7. **Nielsen P.V., Restivo A., Whitelaw J.H.,** The velocity characteristics of ventilated room, J. Fluids Engineering. 100 (3) (1978) 291–298.

8. **Nielsen P.V.,** Specification of a two dimensional test case, Instituttet for Bygningsteknik, Aalborg Universitet, Denmark, Gul Serie, Aalborg. R9040 (8) (1990) 1–15.

9. **Zasimova M.A., Ivanov N.G., Markov D.,** Numerical modeling of air distribution in a test room with 2D sidewall jet. I. Foundations for eddy resolving approach application based on periodical formulation, St. Petersburg Polytechnical State University Journal. Physics and Mathematics 13 (3) (2020) 49–64.

10. **Heikkinen J., Piira K.,** Simulation of simple (two-dimensional) test cases, Technical Research Center of Finland, Laboratory of Heating and Ventilation, Espoo, Finland, Annex report No. AN20.1-SF-91-VTT07 (1991).

11. **Vogl N., Renz U.,** Simulation of simple test cases, In: Energy Conservation in Buildings and in Community Systems, Annex 20. Airflow Patterns within Buildings. No. 1.46. Aachen, Germany, 1991.www.cfd-benchmarks.com.

12. **Skalicky T., Morgenstern G., Auge A., et al.,** Comparative studies of selected discretization methods for the numerical solution of room air flow problems, Proc. of the 3rd International Conference on Air Distribution in Rooms 'ROOMVENT-92' (Aalborg, Denmark, September 2–4, 1992), (1992) 226–240.

13. **Rosler M., Hanel B.,** Numerical computation of flow and heat transfer in air-conditioned rooms by a special velocity-pressure iteration and a multigrid method, Proc. of the 3rd International Conference on Air Distribution in Rooms 'ROOMVENT-92' (Aalborg, Denmark, September 2–4, 1992), (1992) 178–199.

14. **Chen Q.,** Comparison of different k-ε models for indoor air flow computations, J. Numerical Heat Transfer, An International Journal of Computation and Methodology, Part B. Fundamentals. 28 (3) (1995) 353 –369.

15. **Chen Q.,** Prediction of room air motion by Reynolds–Stress models, J. Building and Environment. 31 (3) (1996) 233–244.

16. **Peng S.-H., Davidson L., Holmberg S.,** The two-equation turbulence k-ω model applied to recirculating ventilation flows, Chalmers University of Technology, Sweden, Department of Thermo- and Fluid Dynamics, 1996.

17. **Davidson L., Nielsen P.V.,** Large eddy simulations of the flow in a three dimensional ventilated room, Proc. of the 5th International Conference on Air Distribution in Rooms 'ROOMVENT-96' (Yokohama, Japan, July 17–19, 1996). 2 (1996) 161–168.

18. **Davidson L.,** Implementation of a Large Eddy Simulation method applied to recirculating flow in a ventilated room, Aalborg University, Denmark, Department of Building Technology and Structural Engineering, 1996.

19. **Bennetsen J.C.,** Numerical simulation of turbulent airflow in livestock buildings, The Technical University of Denmark, The Department of Mathematical Modeling, Ph. D thesis, 1999.

20. **Voight L.K.,** Navier – Stokes simulations of airflow in rooms and around human body, International Center for Indoor Environment and Energy, Technical University of Denmark, Department of Energy Engineering, Ph.D thesis, 2000.

21. **Jiang Y., Chen Q.,** Study of natural ventilation in buildings by large eddy simulation, J. of Wind Engineering and Industrial Aerodynamics. 89 (13) (2001) 1155–1178.

22. **Jiang Y., Su M., Chen Q.,** Using large eddy simulation to study airflows in and around buildings, ASHRAE Transactions. 109 (2) (2003) 517–526.

23. **Mora L., Gadgil A.J., Wurtz E.,** Comparing zonal and CFD model predictions of isothermal indoor airflows to experimental data, Indoor Air. 13 (2) (2003) 77–85.

24. **Ivanov N., Smirnov E., Lacor C.,** Computational fluid dynamics analysis of pollutant dispersion in a metro carriage, Proc. of the 17th Air-Conditioning and Ventilation Conference (Prague, Czech. Republic, May 17–19, 2006) (2006) 117–122.

25. **Rong L., Nielsen P.V.,** Simulation with different turbulence models in an annex 20 room benchmark test using Ansys CFX 11.0, Denmark, Aalborg University, Department of Civil Engineering, 2008. DCE Technical Report. No. 46.

26. **Dreau J.L., Heiselberg P., Nielsen P.V.,** Simulation with different turbulence models in an Annex 20 benchmark test using Star-CCM+. Denmark, Aalborg University, Department of Civil Engineering, 2013. DCE Technical Report. No. 147.

27. **Ivanov N.G., Zasimova M.A.,** Large Eddy Simulation of airflow in a test ventilated room // Journal of Physics: Conf. Series. 1038 (2018) 012136.

28. **Ivanov N.G., Zasimova M.A.,** Mean air velocity correction for thermal comfort calculation: assessment of velocity-to-speed conversion procedures using Large Eddy Simulation data, Journal of Physics: Conf. Series. 1135 (2018). 012106.

29. **Yuce B.E., Pulat E.,** Forced, natural and mixed convection benchmark studies for indoor thermal environments, International Communications in Heat and Mass Transfer. 92 (March) (2018) 1–14.

30. **Van Hoof T., Blocken B.,** Mixing ventilation driven by two oppositely located supply jets with a time-periodic supply velocity: A numerical analysis using computational fluid dynamics, Indoor and Built Environment, Special issue – New Building Ventilation Technologies. (November) (2019) 1–18. DOI: 10.1177/1420326X19884667.

31. **Piomelli U.,** Large eddy simulations in 2030 and beyond, Phil. Trans. R. Soc. A. 372 (2022) (2014) 20130320.

32. **Shur M.L., Spalart P.R., Strelets M.K., Travin A.K.,** A hybrid RANS LES approach with delayed-DES and wall-modelled LES capabilities, International Journal of Heat and Fluid Flow. 29 (6) (2008) 1638–1649.

33. **Mathey F.,** Aerodynamic noise simulation of the flow past an airfoil trailing-edge using a hybrid zonal RANS-LES, Computers & Fluids. 37 (7) (2008) 836–843.

Received 20.04.2020, accepted 23.07.2020.

THE AUTHORS

ZASIMOVA Marina A.
Peter the Great St. Petersburg Polytechnic University
29 Politechnicheskaya St., St. Petersburg, 195251, Russian Federation
zasimova_ma@spbstu.ru

IVANOV Nikolay G.
Peter the Great St. Petersburg Polytechnic University
29 Politechnicheskaya St., St. Petersburg, 195251, Russian Federation
ivanov_ng@spbstu.ru

MARKOV Detelin
Technical University of Sofia
8 Kliment Ohridsky boulevard, Sofia, 1000, Bulgaria
detmar@tu-sofia.bg

СПИСОК ЛИТЕРАТУРЫ

1. **Гримитлин М.И.** Распределение воздуха в помещениях. -3е изд., доп. и испр. СПб.: АВОК Северо-Запад, 2004. 320 с.

2. **Рейнольдс О.** Динамическая теория движения несжимаемой вязкой жидкости и определение критерия // Проблемы турбулентности. Сб. переводных статей под ред. М.А. Великанова и Н.Т. Швейковского. Москва-Ленинград: ОНТИ НКТП СССР, 1936. С. 185–227.

3. **Launder B.E., Spalding D.B.** Lectures in mathematical models of turbulence. London, New-York: Academic Press, 1972. 169 p.

4. **Гуляев А.Н., Козлов В.Е., Секундов А.Н.** К созданию универсальной однопараметрической модели для турбулентной вязкости // Известия АН СССР. Механика жидкости и газа. 1993. № 4. С. 69–81.

5. **Sagaut P.** Large Eddy Simulation for incompressible flows: An introduction. 3rd Ed. Heidelberg: Springer, 2006. 556 p.

6. **Гарбарук А.В., Стрелец М.Х., Травин А.К., Шур М.Л.** Современные подходы к моделированию турбулентности. СПб.: Изд-во Политехнического ун-та, 2016. 234 с.

7. **Nielsen P.V., Restivo A., Whitelaw J.H.** The velocity characteristics of ventilated room // J. Fluids Engineering. 1978. Vol. 100. No. 3. Pp. 291–298.

8. **Nielsen P.V**. Specification of a two dimensional test case // Aalborg: Instituttet for Bygningsteknik, Aalborg Universitet, Denmark, Gul Serie. 1990. Vol. R9040. No. 8. Pp. 1–15.

9. **Засимова М.А., Иванов Н.Г., Марков Д.** Численное моделирование циркуляции воздуха в помещении при подаче из плоской щели. I. Отработка применения вихреразрешающего подхода с использованием периодической постановки // Научно-технические ведомости СПбГПУ. Физико-математические науки. 2020. Т. 13. № 3. С. 56–74

10. **Heikkinen J., Piira K.** Simulation of simple (two-dimensional) test cases // Technical Research Center of Finland. Laboratory of Heating and Ventilation. Espoo, Finland. 1991. Annex report. No. AN20.1-SF-91-VTT07. 16 p.

11. **Vogl N., Renz U.** Simulation of simple test cases // Energy Conservation in Buildings and in Community Systems. Annex 20. Airflow Patterns within Buildings. No. 1.46. Aachen, Germany, 1991. 10 p. www.cfd-benchmarks.com.

12. **Skalicky T., Morgenstern G., Auge A., Hanel B., Rosler M.** Comparative studies of selected discretization methods for the numerical solution of room air flow problems // Proc. of the 3rd International Conference on Air Distribution in Rooms 'ROOMVENT-92' (Aalborg, Denmark, September 2–4, 1992). 1992. Pp. 226–240.

13. **Rosler M., Hanel B.** Numerical computation of flow and heat transfer in air-conditioned rooms by a special velocity-pressure iteration and a multigrid method // Proc. of the 3rd International Conference on Air Distribution in Rooms 'ROOMVENT-92' (Aalborg, Denmark, September 2–4, 1992). 1992. Pp. 178–199.

14. **Chen Q.** Comparison of different k-ε models for indoor air flow computations // Numerical Heat Transfer, An International Journal of Computation and Methodology, Part B. Fundamentals. 1995. Vol. 28. No. 3. Pp. 353–369.

15. **Chen Q.** Prediction of room air motion by Reynolds – Stress models // J. Building and Environment. 1996. Vol. 31. No. 3. Pp. 233–244.

16. **Peng S.-H., Davidson L., Holmberg S.** The two-equation turbulence k-ω model applied to recirculating ventilation flows. Chalmers University of Technology, Sweden. Department of Thermo- and Fluid Dynamics. 1996. 26 p.

17. **Davidson L., Nielsen P.V.** Large eddy simulations of the flow in a three dimensional ventilated room // Proc. of the 5th International Conference on Air Distribution in Rooms 'ROOMVENT-96' (Yokohama, Japan, July 17–19). 1996. Vol. 2. Pp. 161–168.

18. **Davidson L.** Implementation of a Large Eddy Simulation method applied to recirculating flow in a ventilated room. Aalborg University, Denmark. Department of Building Technology and Structural Engineering. 1996. 28 p.

19. **Bennetsen J.C.** Numerical simulation of turbulent airflow in livestock buildings. The Technical University of Denmark. The Department of Mathematical Modeling. Ph. D thesis. 1999. 205 p.

20. **Voight L.K.** Navier – Stokes simulations of airflow in rooms and around human body. International Center for Indoor Environment and Energy, Technical University of Denmark. Department of Energy Engineering. Ph.D thesis. 2001. 169 p.

21. **Jiang Y., Chen Q.** Study of natural ventilation in buildings by large eddy simulation // J. of Wind Engineering and Industrial Aerodynamics. 2001. Vol. 89. No. 13. Pp. 1155–1178.

22. **Jiang Y., Su M., Chen Q.** Using large eddy simulation to study airflows in and around buildings // ASHRAE Transactions. 2003. Vol. 109. No. 2. Pp. 517–526.

23. **Mora L., Gadgil A.J., Wurtz E.** Comparing zonal and CFD model predictions of isothermal indoor airflows to experimental data // Indoor Air. 2003. Vol. 13. No. 2. Pp. 77–85.

24. **Ivanov N., Smirnov E., Lacor C.** Computational fluid dynamics analysis of pollutant dispersion in a metro carriage // Proc. of the 17th Air-Conditioning and Ventilation Conference (Prague, Czech. Republic, May 17–19, 2006). 2006. Pp. 117–122.

25. **Rong L., Nielsen P.V.** Simulation with different turbulence models in an annex 20 room benchmark test using Ansys CFX 11.0. Denmark, Aalborg University, Department of Civil Engineering, 2008. DCE Technical Report. No. 46. 16 p.

26. **Dreau J.L., Heiselberg P., Nielsen P.V.** Simulation with different turbulence models in an Annex 20 benchmark test using Star-CCM+. Denmark, Aalborg University, Department of Civil Engineering, 2013. DCE Technical Report. No. 147. 22 p.

27. **Ivanov N.G., Zasimova M.A.** Large Eddy Simulation of airflow in a test ventilated room // Journal of Physics: Conf. Series. 2018. Vol. 1038. International Conference PhysicA.SPb/2017, 24–26 October 2017, Saint-Petersburg, Russia. P. 012136.

28. **Ivanov N.G., Zasimova M.A.** Mean air velocity correction for thermal comfort calculation: assessment of velocity-to-speed conversion procedures using Large Eddy Simulation data // Journal of Physics: Conf. Series. 2018. Vol. 1135. International Conference PhysicA.SPb/2018, 23–25 October 2018, Saint-Petersburg, Russia. P. 012106.

29. **Yuce B.E., Pulat E.** Forced, natural and mixed convection benchmark studies for indoor thermal environments // International Communications in Heat and Mass Transfer. 2018. Vol. 92. March. Pp. 1–14.

30. **Van Hoof T., Blocken B.** Mixing ventilation driven by two oppositely located supply jets with a time-periodic supply velocity: A numerical analysis using computational fluid

dynamics // Indoor and Built Environment. 2019. Special issue – New Building Ventilation Technologies. November. Pp. 1–18. DOI: 10.1177/1420326X19884667.

31. **Piomelli U.** Large eddy simulations in 2030 and beyond // Phil. Trans. R. Soc. A. 2014. Vol. 372. No. 2022. P. 20130320.

32. **Shur M.L., Spalart P.R., Strelets M.K., Travin A.K.** A hybrid RANS-LES approach with delayed-DES and wall-modelled LES capabilities // International Journal of Heat and Fluid Flow. 2008. Vol. 29. No. 6. Pp. 1638–1649.

33. **Mathey F.** Aerodynamic noise simulation of the flow past an airfoil trailing-edge using a hybrid zonal RANS-LES // Computers & Fluids. 2008. Vol. 37. No. 7. Pp. 836–843.

Статья поступила в редакцию 20.04.2020, принята к публикации 23.07.2020.

СВЕДЕНИЯ ОБ АВТОРАХ

ЗАСИМОВА Марина Александровна – *ассистент Высшей школы прикладной математики и вычислительной физики Санкт-Петербургского политехнического университета Петра Великого.*
195251, Российская Федерация, г. Санкт-Петербург, Политехническая ул., 29
zasimova_ma@spbstu.ru

ИВАНОВ Николай Георгиевич – *кандидат физико-математических наук, доцент Высшей школы прикладной математики и вычислительной физики Санкт-Петербургского политехнического университета Петра Великого.*
195251, Российская Федерация, г. Санкт-Петербург, Политехническая ул., 29
ivanov_ng@spbstu.ru

МАРКОВ Детелин – *PhD, доцент Софийского технического университета.*
1000, Болгария, г. София, бульвар Климента Орхидского, 8
detmar@tu-sofia.bg